This document was prepared in conjunction with work accomplished under Contract No. DE-AC09-96SR18500 with the U. S. Department of Energy.

DISCLAIMER

Proceedings of PVP2006-ICPVT-11
2006 ASME Pressure Vessels and Piping Division Conference
July 23-27, 2006, Vancouver, BC, Canada

PVP2006-ICPVT11-93523

APPLICATION OF A DYNAMIC STRESS THEORY TO PIPE LEAKS

Robert A. Leishear
Westinghouse Savannah River Corporation
Aiken, South Carolina, 29808
803-208-8394, Robert.Leishear@SRS.gov

ABSTRACT

Leaks in system piping used to transfer radioactive waste were attributed to water hammer. Valves leaked on several occasions and the cause of failure was not obvious. Facility records were used to determine the facility status at the time the leaks occurred. For one particular leak, valve manipulations controlling flow were shown to be coincident to the time of leak. The fluid transient pressures were calculated using TFSIM from the Tennessee Valley Authority. Once the maximum pressures were established, the stresses on the equipment could be discerned. Water hammer was concluded to be the failure mechanism. To eliminate this failure mechanism, procedural and equipment modifications were made and further leaks have been eliminated.

NOMENCLATURE

D	damping factor, psi
Δh	change in enthalpy, BTU / pound
Δs	change in entropy, BTU / pound·°R
E	elastic modulus, psi
ft	feet
h	enthalpy, BTU / pound
HDB4-6	diversion box
i	dynamic amplification factor
NPS	national pipe schedule
psi	pounds per square inch
P, P_{eq}	pressure, psi
PI	Process Information systems
s	entropy, BTU / pound·°R
SRS	Savannah River Site
St	static stress, psi
T_0	temperature, °R
TFSIM	Transient Fluid Simulation
σ	dynamic stress, psi
σ_e	fatigue limit, psi
σ_{ra}	range stress, psi
ν	Poisson's ratio
ζ	damping ratio
ζ_{fl}	fluid damping ratio
ζ_s	structural damping ratio

INTRODUCTION

A recently developed dynamic stress theory (Leishear [1]) is applied here to evaluate valve failures in a piping system. In particular, valve leakage in a Savannah River Site (SRS) nuclear waste transfer system occurred during three separate incidents. In each incident, the waste was safely contained. However, a detailed analysis was performed to determine the failure cause. To perform the analysis, a description of the system, a description of the affected processes, and a fluid transient analysis are prerequisite to an evaluation of the stresses imposed on valves in the system and the implemented solutions to the problem. Essentially, a detailed description of the water hammer incidents and damages are followed by a pipe stress analysis and corrective actions.

SYSTEM DESCRIPTION

A system description is the basis for a system model, and the system in question consists of two connected piping systems: the flush water system and the transfer system. The flush water system provides water to flush, or rinse, the transfer piping after nuclear waste has been transported through the transfer piping. The flush water is connected to the transfer system through closed valves, which are opened to flush the transfer piping on completion of a transfer. There are numerous transfer lines and flush water systems at SRS, but this study was limited to one section of transfer piping and the flushes needed to effectively remove the waste from that transfer line. At the time the valves leaked, the transfer piping was operated in tandem with the flush water system. The focus of this paper is the relationship between valve failures and fluid transients, or pressure surges, induced by the flush water system which is described by the system description below.

System Schematic

A schematic of the combined transfer and flush water system is shown in Fig. 1. The facility layout and the pertinent flush water flow paths are shown in Fig. 2. Some added discussion clarifies the flush water system layout. The flow initiates within the 242-11H building at the flush water tank (Fig. 3), passes down through the flush water pump (Fig. 4), exits the building, and circles Tank 37, which is a nuclear waste storage tank. On the west side of Tank 37, the pipe tees off to Tank 37 in one direction. The piping continues to circle Tank 37 in the other direction to HDB6 and Tank 32. The underground transfer lines

connected between the diversion boxes and waste Tanks 32 and 37 are shown schematically in Fig. 5. Diversion boxes, like HDB6, are below grade concrete structures containing valves used to divert, or change, the flow path in the waste transfer piping system. HDB6 and HDB4 are shown in Figs. 6 and 7 respectively and are both shown in Fig. 2.

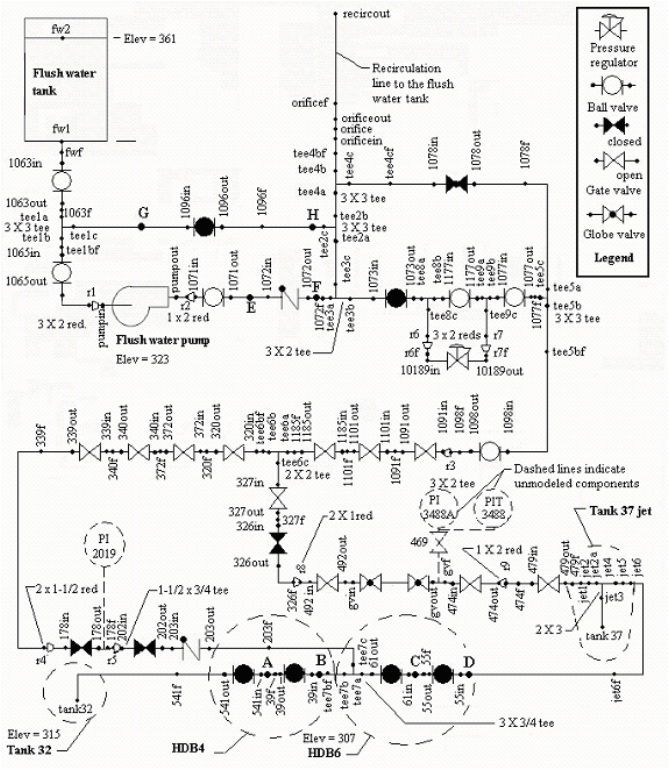

Figure 1: System Model / Schematic

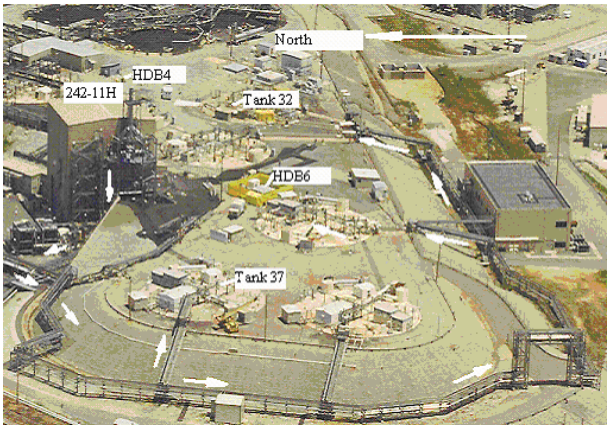

Figure 2: System Layout

Figure 3: Flush Water Tank

Figure 4: Flush Water Pumps

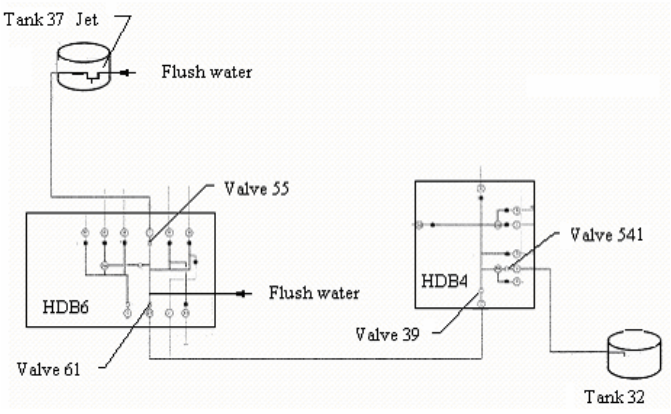

Figure 5: Schematic of Transfer Lines Between Tanks 32 and 37

Figure 6: HDB6

HDB4 cover and valve handles to operate valves

Valves and piping inside HDB4

Figure 7: HDB4

PROCESS DESCRIPTION

There were three separate incidents of valve leakage in the transfer piping. During each incident several flow paths were used to flush the transfer lines. The various process flow paths are presented in Figs. 8 – 11 and were extracted from Fig. 1. In each of these flow paths a single valve was suddenly opened while the pump was operating. This action induced water hammers, or fluid transients, of varying magnitudes throughout the system. Each of the figures shows all of the piping which was in service at the time when the successive water hammers occurred.

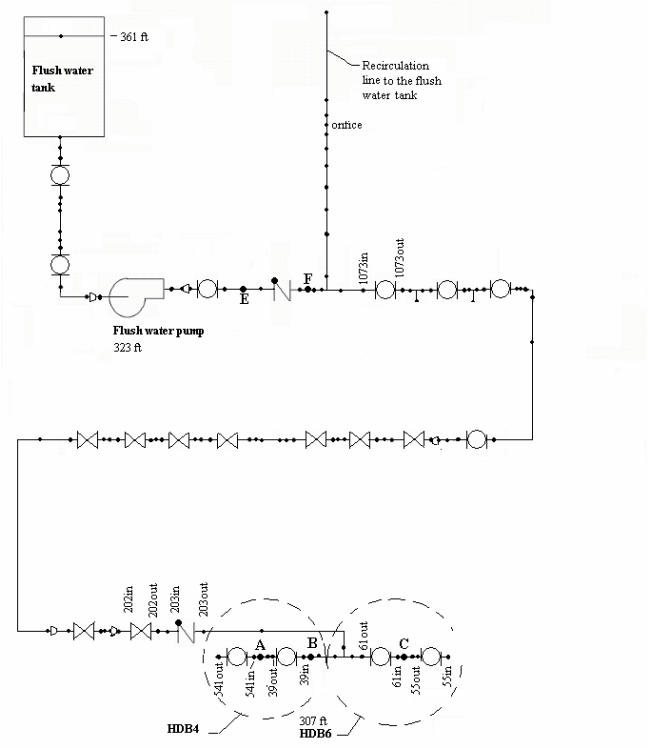

Figure 8: Schematic for Flush Water Pump Operation

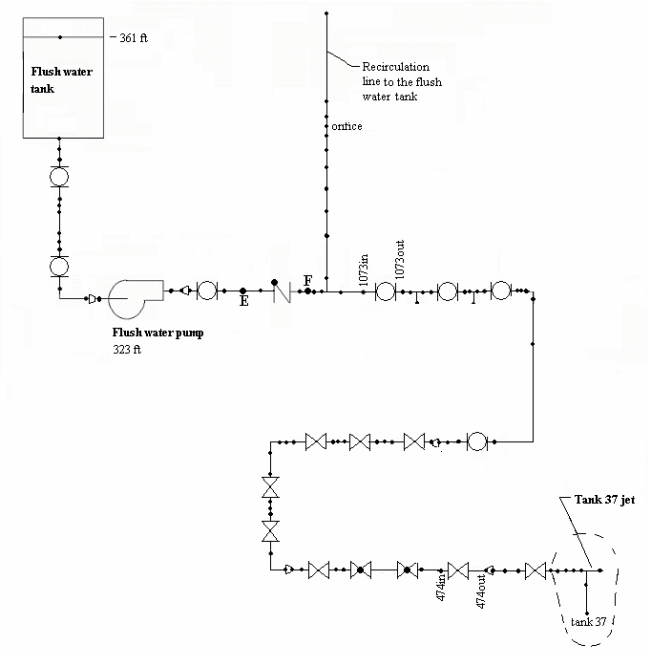

Figure 9: Modeled Flow Path for Tank 37 Jet Flush

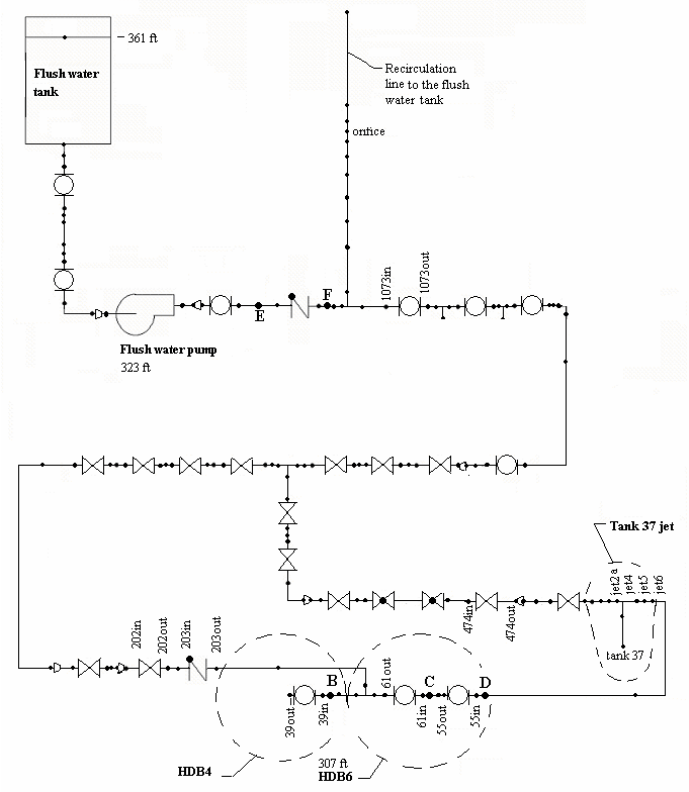

Figure 10: Modeled Flow Path for HDB6 Flush

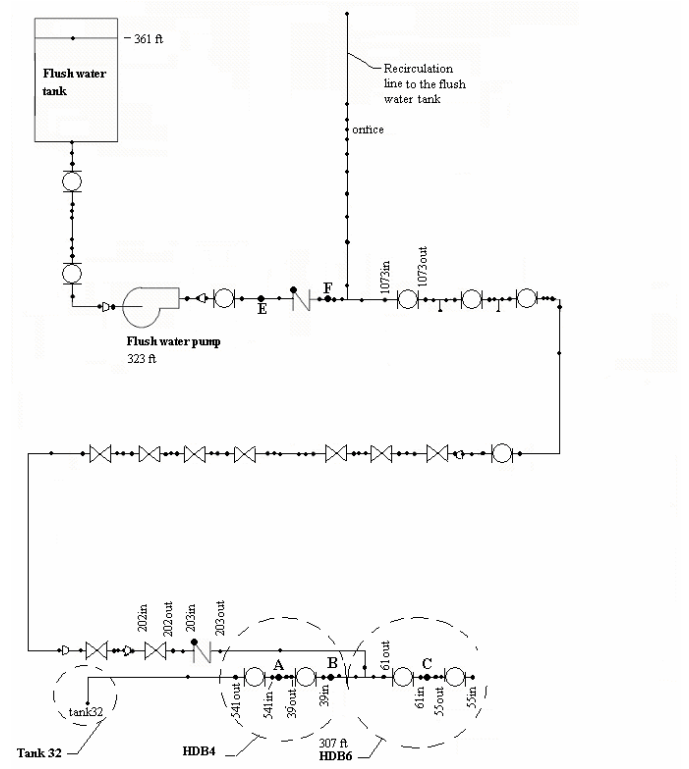

Figure 11: Modeled Flow Path for the HDB4 Flush

RECORD OF VALVE LEAKAGE

One of the valve leaks occurred at HDB4 and the system performance was recorded at the time that leak occurred. System records are kept in the facility using the Process Information System(PI [2]). The record of this incident is shown in Fig. 12. The figure is annotated to depict the times at which the various flushes were implemented.

The legend in the lower left hand corner of the figure provides the key to observe the flush tank level. EVP FLW TANK LEVEL indicates the level in the tank as the flushes are performed. The tank level varies between 25 and 45 inches, where the tank level is recorded on the right hand side of the graph. Note that the flush tank level varies rapidly between the points indicated as points 2 – 11 on the graph. At these times, flushes are being performed and the tank is being continually emptied and refilled.

The sump level indicates the actual occurrence of the leak. As the valve leaked into the diversion box (HDB4), a depression in the floor of the diversion box, called a sump, collected the leaked waste, and the level in the sump was recorded. This level is shown in Fig. 12 and can be seen to vary between 2 and 10 inches. The magnitude of the level is discerned from the scale at the right side of the graph. The leak started at point 2 shown on the graph when one of the water hammers damaged the valve. At point 12 on the graph, the valves were hammered again and the leak rate increased. At point 13, the sump was emptied using a remotely operated jet eductor pump, which is installed in the sump. The time scale on the bottom of the graph shows that the entire incident occurred in less than one hour. The size of the leak during this time was approximately seven gallons. The leaking nuclear waste was completely contained within the diversion box. In short, leaks were coincident to valve manipulations. The relationship of these valve manipulations to water hammer are considered next.

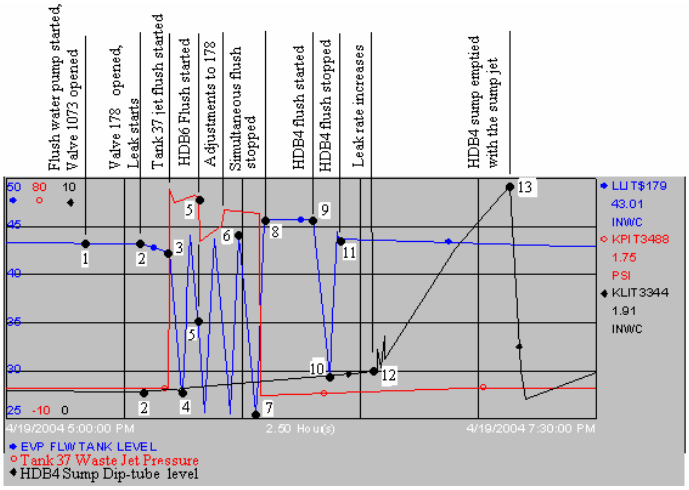

Figure 12: Documentation of HDB4 Leak Using PI

WATER HAMMER CALCULATIONS

The magnitudes of the pressure transients were calculated using TFSIM (Schohl [3])and the model shown in Fig. 1.The details of the fluid flow analysis are available and the results of those calculations are considered to be accurate to within 10 to 30 percent (Leishear [4]). Those calculations are summarized by redrawing Fig. 12 as Fig. 13 and annotating the graph with TFSIM results. The figure shows the various

surges which occurred during each of the three leaks. Note that the pressure surges varied from 300 to 524 psi. Having determined the system pressures, the failure mechanism of the valve was considered.

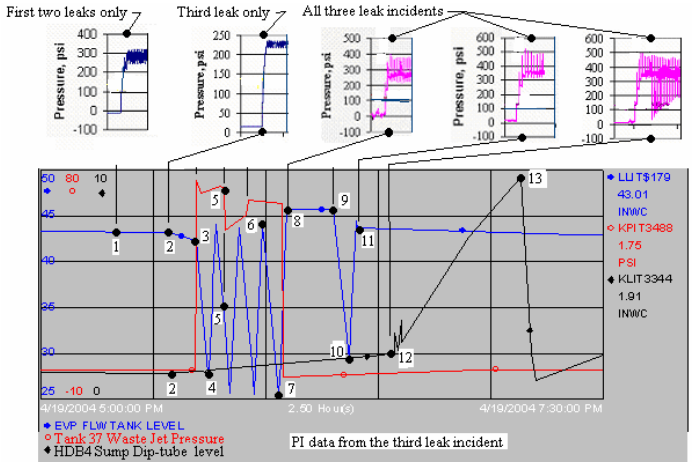

Figure 13: Summary of Transient Pressures Causing Leaks

VALVE FAILURE MECHANISM

The valve leaked around the valve stem as shown in Fig. 14. This figure provides a photograph of the valve leakage and an enlargement of that photograph. The stem connects the ball inside the valve to the handle mounted above the diversion box shown in Fig. 7. The valves are rated to 760 psi and one valve was hydrostatically tested to 1000 psi as shown in Fig. 15. The pressure was slowly applied in the hydrostatic test. However, the applied pressures of 300 – 524 psi during the water hammers were suddenly applied, and dynamic effects must therefore be considered since the applied pressures are below the rated pressures of the valve.

Figure 14: Photographs of Transfer Valve Packing Leak

Figure 15: Hydrostatic Test of a Valve Identical to the Leaking Valve

DYNAMIC EFFECTS OF THE APPLIED PRESSURE

The dynamic effects of a suddenly applied pressure are available in earlier work (Leishear [1]). All of the equations used below in this dynamic analysis were presented and discussed in detail in this earlier work. The dynamic stress, σ, was shown to be a function of the static stress due to a gradually applied load, St, Poisson's ratio, ν, and a dynamic amplification factor, i. For a short length of pipe the maximum hoop stress equals

$$\sigma = i \cdot St < 2 \cdot St \quad (1)$$

For a long length of pipe, the hoop stress equals

$$\sigma = i \cdot St < (3 + \nu^2) \cdot St \quad (2)$$

Substitution of Eq. 1 into Eq. 2 yields

$$\sigma = (\frac{3 \cdot i}{2} + \nu^2) \cdot St < (3 + \nu^2) \cdot St \quad (3)$$

This equation can be used to find the hoop stress in a long length of continuous pipe, but how can this equation be applied to a valve, which does not have a cylindrical shape? Equation 1 is applicable to any shape and can be directly applied by using an equivalent pressure P_{eq}. Since the static and dynamic stresses are proportional to the applied pressure, P.

$$(\frac{3 \cdot i}{2} + \nu^2) \cdot P \geq P_{eq} \geq i \cdot P \quad (4)$$

P_{eq} is greater than or equal to $i \cdot P$ since it lies somewhere between the values prescribed by Eqs. 1 and 3. The exact values of P_{eq} can only be found for a valve on a case by case basis using finite element techniques. Having obtained Eq. 4, the value of i needed to be determined to complete a failure analysis of the valve.

Dynamic Analysis of the Failure

The pressures shown in Fig. 13 were approximated in this analysis by a single step pressure increase of 524 psi. This approximation provides a bounding upper limit to this analysis. The equivalent pressure equals

$$P_{eq} = P \cdot \left(1 + e^{\left[\frac{-\zeta \cdot \pi}{\sqrt{1-\zeta^2}} \right]} \right) = P \cdot i \quad (5)$$

The damping coefficient for a vibrating system, ζ, is found from the fluid damping, ζ_{fl}, and the structural damping, ζ_S.

Fluid damping. The fluid damping has the greatest effect on the pipe stress solutions. The second law of thermodynamics and the vibration equations can be combined to find a minimum damping coefficient due to fluid damping. Figs. 16 and 17 facilitate discussion of this concept.

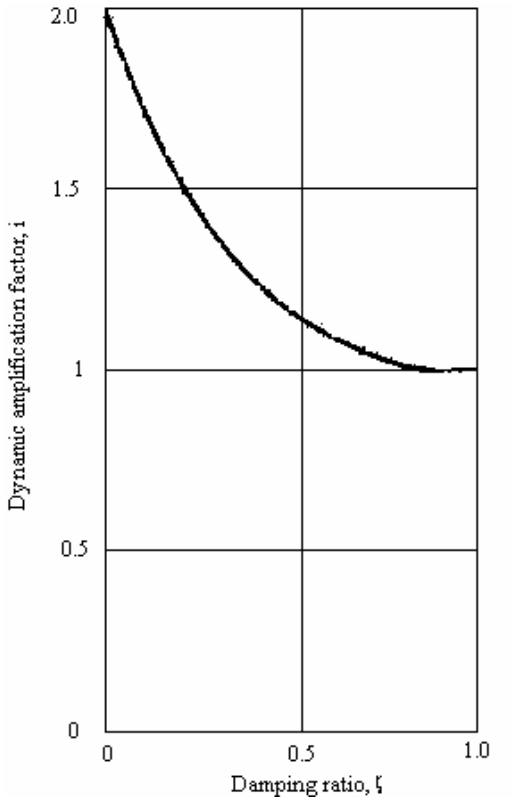

Figure 16: Dynamic Amplification Factor

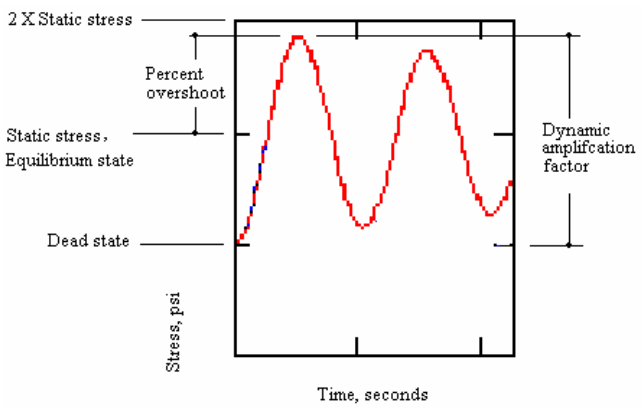

Figure 17: Relationship Between Dynamic Amplification Factor and Thermodynamic Efficiency

The percent overshoot, PO, is the percentage of increase above the static stress that occurs when a step pressure is exerted on the pipe wall, and can be expressed as

$$PO = \left(e^{\left[\frac{-\zeta \cdot \pi}{\sqrt{1-\zeta^2}} \right]} \right) \tag{7}$$

In the absence of damping, the PO equals one. Simply adding this value to one gives the dynamic amplification factor for the SDOF model, which typically varies between one and two.

$$i = \left(1 + e^{\left[\frac{-\zeta \cdot \pi}{\sqrt{1-\zeta^2}} \right]} \right) \tag{8}$$

The Second Law thermodynamic efficiency may be defined as the maximum work that can be obtained from a system. For a compression cycle, the efficiency equals

$$\varepsilon = \frac{\Delta h - \left| T_0 \cdot \Delta s \right|}{\Delta h} \tag{9}$$

where Δh is the change in enthalpy or ideal work of the process, Δs is the change in entropy, and T_0 is the ambient temperature. The thermodynamic properties are obtained at the initial or dead state, and the final, or equilibrium state. Assuming the fluid properties to vary linearly, and considering only fluid damping, the maximum achievable stress must, of necessity, be governed by this Second Law relationship. In that case, the maximum stress equals

$$\sigma = \varepsilon \cdot \sigma_{max} = \varepsilon \cdot 2 \cdot St = i \cdot St \tag{10}$$

and the dynamic amplification factor, i, is expressed by

$$2 \cdot \varepsilon = i \tag{11}$$

Using Eq. 7 and 10, the fluid damping can be determined. There may be other losses associated with cavitation at the pipe wall / fluid interface, but, at a minimum, this fluid damping coefficient should be considered. Once the fluid damping coefficient is established, the lesser structural damping coefficient can be considered.

Equating the dynamic amplification factor to one half of the thermodynamic efficiency, ε, the damping coefficient, ζ, can be found. The values for the entropy, s, and enthalpy, h, are first required for this comparison. The dead state is 14.7 psi, and the equilibrium state occurs at the median pressure, 524 + 14.7 ≈ 539 psi. The required values of the enthalpy, h, and the entropy, s, are found in the steam tables (Keenan, et. al. [5]), using linear interpolation. T_0 is the ambient temperature.

The efficiency then equals

$$\varepsilon = \frac{(39.51 - 38.06) + (459 + 70) \cdot (0.07331 - 0.07348)}{(39.52 - 38.06)} = .932 \tag{12}$$

Pressure psi	0	14.7	500	564	1000
Temp. °F	h, from steam table	*Δh BTU/ (pound)*	h, from steam table	*Δh BTU/ (pound)*	h, from steam table
50	18.06		19.50		20.94
70		*38.06*	39.44	*39.55*	40.84
100	68.05		69.36		70.68
	s, from steam table	*Δs BTU/ (pound°R)*	s, from steam table	*Δs BTU/ (pound°R)*	s, from steam table
50	-.03607		0.03599		0.03592
70	0.07349	*0.07348*	0.07332	*0.07329*	0.07316
100	0.12963		0.12932		0.12901

Table 2: Calculation of Enthalpy and Entropy

Substitution of Eq. 11 into Eq. 8, and Solving for ζ_{fl}, yields

$$\zeta_{fl} = \sqrt{\frac{2 \cdot (\ln(0.932 - 1))^2}{(\ln(0.932 - 1))^2 + \pi^2}} = 0.066 \tag{13}$$

Having obtained the fluid damping factor, the effects of structural damping were also considered.

Structural damping. The structural damping coefficient, ζ_S, was calculated using Lazan's [6] approximation for the damping ratio (Eq. 11) was based on a number cycles equal to $2 \cdot 10^7$ cycles. For this number of cycles, the value for the endurance strength, or fatigue limit, of TP304L stainless steel is 24,300 psi. the fatigue strength is extrapolated from the ASME Boiler and Pressure Vessel Code, Sect. III, Table I-9.2.2, Curve A. Then,

$$\sigma_e = 24700 psi \tag{14}$$

$$D = \left(\frac{\sigma_{ra}}{\sigma_e} \right)^{2.4} + 6 \cdot \left(\frac{\sigma_{ra}}{\sigma_e} \right)^8$$

$$= \left[\left(\frac{7514}{24300} \right)^{2.4} + 6 \cdot \left(\frac{7514}{24300} \right)^8 \right] = 0.0602 psi \tag{15}$$

$$\zeta_S = \frac{D \cdot E}{2 \cdot \pi \cdot \sigma_{ra}^2} = \frac{0.0602 psi \cdot 30800000 psi}{2 \cdot \pi \cdot 7514^2 psi^2} = 0.0052 \tag{16}$$

where D is a material property known as the damping factor, and E is the Modulus of Elasticity.

Total damping. This 0.52 % damping value is in the range of the value of 2 % required for ASME B31.3 piping which has a diameter less than 12 inches. The ASME values are used for the structural response of piping during earthquakes. The value of ζ_S, equal to 0.5 % value was used in this calculation. Assuming the principle of superposition, the damping coefficients are added to obtain

$$\zeta \cong \zeta_{fl} + \zeta_S = 0.066 + 0.005 = 0.071 \qquad (17)$$

Damping factor and equivalent pressure. Although a trial and error solution could be used to refine the value of the damping coefficient, a reasonable approximation of the equivalent pressure is

$$P_{eq} = 524\text{psi} \cdot \left(1 + e^{\left[\frac{-0.071 \cdot \pi}{\sqrt{1 - 0.071^2}} \right]} \right) = P \cdot i = 1.8 \cdot P = 943\text{psi} \qquad (18)$$

The dynamic amplification factor is then

$$i = 1.8 \qquad (19)$$

This value of i is applicable to the case where the maximum pressure in the pipe was found to be 524 psi. Since this was the largest pressure calculated in this analysis, and i is proportional to stress, values of i for lower pressures will be less than this value. That is, i < 1.8. The equivalent pressure of 943 psi is beyond the design limit of 760 psi for the valves, and as noted above, the effects of the pressure may be even greater than the 943 psi value.

CORRECTIVE ACTIONS

Facility procedures and equipment were modified and further damage was eliminated. Immediate changes were made to procedures and personnel training to control transients in this system. A slow operating valve was also installed to eliminate significant transients. TFSIM was used to evaluate the effectiveness of the slow acting valve. Figure 8 and Fig. 18 describe the same water hammer event. The only difference between the two figures is that Fig. 18 has been simplified and annotated with TFSIM results. Figure 19 provides the TFSIM results for this same configuration where the transient is controlled with a ball valve having a ten second linear closure time. A comparison of Figs. 18 and 19 shows that the transients are very well controlled using this technique. Other transients were controlled procedurally.

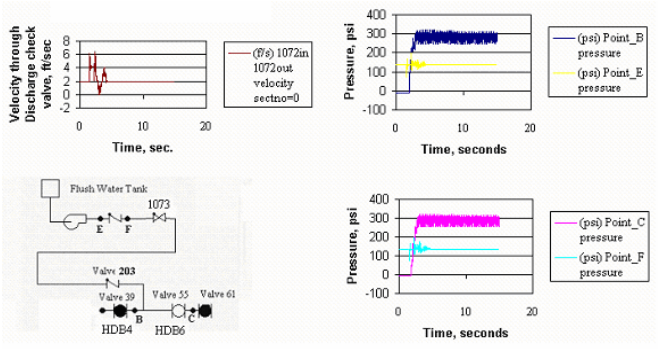

Figure 18: Pressure increase when Valve 1073 is Suddenly Closed

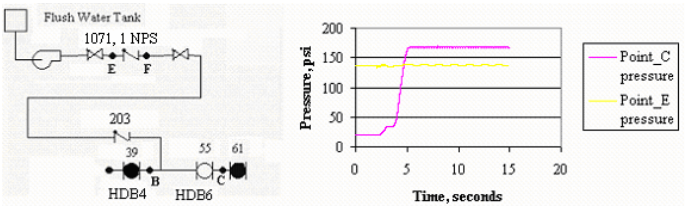

Figure 19: Pressure Increase when a Linear Actuated Ball Valve is used to Control Fluid Transients

CONCLUSION

Did the valve leaks result from water hammer? The facts indicate yes. Three separate leaks occurred during flushing operations. The third leak is well documented. The initial leak occurred when valves were operated, several hundred feet away. This paper quantifies a pressure surge occurred, which occurred when the valves were operated, and proves that water hammer was the initiating event for the failure. More importantly, the use of a dynamic amplification factor was used to investigate pipe failures due to a suddenly applied load caused by water hammer. The most complex part of a water hammer analysis is the fluid transient analysis. The pipe stresses or equivalent pressures in a piping system can be reasonably approximated using recently published closed form solutions.

REFERENCES

[1] Leishear, R. A., 2005, "Dynamic Stresses During Structural Impacts and Water Hammer", PhD Dissertation, University of South Carolina, pp.1- 188.

[2] "Plant Information Systems", 2000, OSI Software Inc., San Leandro, Cal.

[3] Schohl, G., 1998, "Users Manual for Locksim, Hydraulic Simulation of Navigation Lock Filling and Emptying Systems", Tennessee Valley Authority, pp.1 – 191.

[4] Leishear, R. A., 2006, "Water Hammer Evaluation for the H Area Tank Farm, West Hill Flush Water System", WSRC-TR-2006-00091, Washington Savannah River Corp., South Carolina, pp. 1 – 137.

[5] Keenan, J. H., Keyes, F. G., Hill, P. G., and Moore, J. G., 1969, *Steam Tables*, Wiley, N. Y, p. 104.

[6] Lazan., B. J., 1975, "Energy Dissipation Mechanisms in Structures, with Particular Reference to Material Damping", *Structural Damping*, ASME, N. Y., pp. 1 - 34.